IET Generation, Transmission & Distribution

Research Article

IET Journals
The Institution of Engineering and Technology

Fault location estimator for series compensated transmission line under power oscillation conditions

ISSN 1751-8687
Received on 21st August 2015
Revised on 25th November 2015
Accepted on 13th April 2016
doi: 10.1049/iet-gtd.2015.1017
www.ietdl.org

Yujia Deng, Zhengyou He ✉, *Ruikun Mai, Sheng Lin, Ling Fu*

School of Electrical Engineering, Southwest Jiaotong University, Chengdu 610031, People's Republic of China
✉ *E-mail: hezy@swjtu.cn*

Abstract: This study proposed a novel fault-location algorithm for a series capacitor (SC) compensated transmission lines under power oscillation conditions. Synchronous voltage and current phasors from both terminals of the transmission line are employed to estimate the fault location while considering the distributed parameter line model. An iterative method is proposed to obtain the voltage across the SC under power oscillation conditions. The fault-location algorithm includes three stages. Firstly, the distributed parameters of the transmission line are estimated by the dynamic parameters estimate method. Secondly, the voltage of the SC can be solved by the iterative method based on the phasor measurements and the transmission line parameters. Finally, the fault location can be attained via Newton iteration method. A 300 km/500 kV transmission compensated by SC simulated in PSCAD/EMTDC has been employed to evaluate the performance of the proposed algorithm under various power oscillation situations. The simulations have demonstrated that the proposed method independent of fault types, fault resistance and fault distances under power oscillation conditions. The accuracy of the proposed algorithm is far higher than that of the conventional fault location algorithms in most cases.

1 Introduction

The installation of the series compensation device on transmission system is an effective way to compensate line reactance, to enhance power system's stability, shorten the electrical distance and improve power transfer capability [1, 2]. However, since the series compensation devices undermine the continuity of the line parameters and the variation of series compensation voltage remains uncertain during the fault period it brings new challenges to fault location. Besides, accurate fault location is of great significance for power utilities to expedite line restoration, reduce the outage time and avoid power systems entering unstable state [3].

Conventional transmission fault location algorithms dealing with series capacitor (SC) compensated conditions can be classified as follows: single-end fault-location algorithm [4, 5] and two-end fault-location algorithm [6], travelling wave-based algorithm [7] and artificial neural networks (ANNs)-based algorithm [8, 9]. The main limitation of travelling wave-based algorithm is the high sampling frequency, and the performance of ANN-based algorithm directly depends on its training process and its predefined structure. The single-end algorithm is seriously affected by fault resistance in comparison with two-end fault-location algorithms. Ever since the electromagnetic time-reversal theory has been employed to locate fault [10], the accuracy of fault location based on single-end information for series compensated transmission have been improved a lot [5]. However, the fault resistance is also one of the most concerned problems for single-end algorithm. For the two-end fault-location algorithms, how to reduce and eliminate the influence of the series compensation device is one of the most concerned issues, since inaccurate estimation of the voltage drop across the series compensation device will affect the performance of the fault location algorithms. These algorithms can be divided into two categories [11] depending on whether considering the voltage drop of the series compensation device or not. The equivalent models of series compensation device were used to calculate the voltage drop [12, 13]. An optimised algorithm is proposed to estimate the fault location to avoid the disadvantages of iteration-based algorithm [12]. A correction step is put forth to calculate voltage drop of the series compensation device [13], and obtain the fault distance via iteration and correction. For the sake of avoiding the effect of iteration, a non-iterative fault location algorithm based on two-end unsynchronised measurements is proposed [14]. Furthermore, more accurate phasors estimation methods are proposed based on Pony analysis and discrete Fourier transform in order to gain higher precision [15, 16]. A series of fault location algorithms based on fault loop are proposed [17], which are independent of the knowledge of the series compensation device. The two-terminal current and one-terminal voltage are utilised to calculate the fault location [18], and reduce the impact of the series compensation device. All of these algorithms have a great significance to improve the accuracy of fault location, but ignored the power oscillation conditions.

In general, rapid power oscillation occurs because power systems often operate close to the stability boundary for economic purposes [19, 20]. Besides, the change in the configuration and loading of system causes a power swing between the load concentrations of the network [21–23]. During this period, the frequencies of power system are changing relatively fast. However, all of the algorithms mentioned above are considered the power system operates in a static condition, which significantly reduce the accuracy of fault localisation during power oscillation. A dynamic synchrophasor estimation algorithm is introduced to improve the estimation accuracy under dynamic conditions [24, 25]. Based on these, a series of fault location algorithm under dynamic conditions are proposed to overcome the influence of dynamic condition [26, 27], which offer more advantages than conventional methods. These algorithms are able to express the dynamic characteristics of power systems in spatial span as well as in time scale, and give accurate estimation of fault location under different dynamic conditions, but fail to be applied to series compensated lines.

In this paper, an approach for fault location in a SC compensated transmission line under dynamic conditions is proposed. The method of dynamic parameter estimator [26] is used. The iterative method is employed to modify the voltage drop of the series compensation device, which is the main contribution of this paper. In the proposed method, the series compensation device is considered as a series capacitor.

The rest of this paper is organised as follows: Section 2 introduces the principle of the novel fault location method. The evaluation of the proposed method using PSCAD/EMTDC which generated signals based on a faulted SC compensated line is presented in Section 3. Last but not least, Section 4 is the conclusion.

2 Principle of the new fault location algorithm

A single-phase SC compensated transmission line is shown in Fig. 1. M and N denote the sending and receiving ends, respectively. Without loss of generality, a fault appears at right-hand side of the series compensator as shown in Fig. 1*a*, or the left-hand side of the series compensator as shown in Fig. 1*b*. x denotes the fault distance away from the terminal which is close to the fault point F. The series compensator is mounted between M and N. l is the length of the transmission line, and k represents the percentage of compensator of the transmission line, where $0 \le k \le 1$.

Synchronous voltage and current phasors from both ends of the transmission line are adopted by the proposed algorithm. The current and the voltage of point E ($\dot{U}_E$, $\dot{I}_E$) can be calculated using the voltage and current of terminal M ($\dot{U}_M$, $\dot{I}_M$) [28] if the fault occurs at the right-hand side of SC. The current of point B ($\dot{I}_B$) is equal to $\dot{I}_E$, and the voltage of point B ($\dot{U}_B$) can be obtained

$$\dot{U}_B = \dot{U}_E - \dot{U}_S \tag{1}$$

where $\dot{U}_S$ is the voltage across the SC, and it can be expressed as

$$\dot{U}_S = \dot{I}_S \cdot \frac{1}{j\omega_0 C_s} \tag{2}$$

where $\dot{I}_S$ is the current flowing through the SC, ω_0 is the angular velocity and C_s is the capacitance of SC.

Regarding the section BN as a transmission line without the SC, and the conventional two-terminal fault-location algorithm can be applied since the information of point B and terminal N are available. Theoretically, the more accuracy of the information, the more accuracy of the fault location's result. However, the method solving the $\dot{U}_B$ does not get enough credit for the precision under fast power oscillation condition because of the frequency is changing. From this aspect, a method to correct the $\dot{U}_B$ is proposed.

In this paper, it is assumed that the fault section is already known [29], and for convenience of description, fault occurs at the right-hand side of the SC as an example to illustrate the principle. The left-hand side can deal with as same as the right-hand side. In the following text, the static-fault locator algorithm is illustrated firstly based on the distributed parameter line. Then, the dynamic-fault location algorithm including the iteration method is introduced.

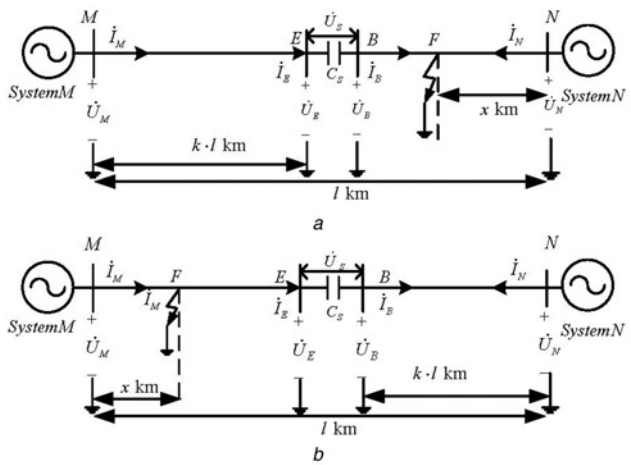

Fig. 1 *Circuit diagrams of series-compensated transmission line with a fault on the*

a Right-hand side of the compensator
b Left-hand side of the compensator

2.1 Static-fault locator algorithm for transmission line

Based on the distributed parameter model of transmission line, it is easy to obtain the voltage and current at a distance x from the terminal N [28]

$$\dot{U} = \dot{U}_N \cdot \cosh(\gamma \cdot x) - \dot{I}_N \cdot Z_C \cdot \sinh(\gamma \cdot x) \tag{3}$$

$$\dot{I} = -\frac{\dot{U}_N}{Z_C} \cdot \sinh(\gamma \cdot x) + \dot{I}_N \cdot \cosh(\gamma \cdot x) \tag{4}$$

where $Z_C = \sqrt{Z/Y}$, which is the characteristic impedance per unit length and $\gamma = \sqrt{Z \cdot Y}$, which is the propagation constant per unit length. Z is the impedance per unit length. Y is the admittance per unit length.

Since the hyperbolic function can be defined by the exponential function, (3) and (4) can be expressed as [30]

$$\dot{U} = \frac{\dot{U}_N - \dot{I}_N Z_C}{2} e^{\gamma x} + \frac{\dot{U}_N + \dot{I}_N Z_C}{2} e^{-\gamma x} \tag{5}$$

$$\dot{I} = \frac{(\dot{U}_N/Z_C) - \dot{I}_N}{2} e^{\gamma x} - \frac{(\dot{U}_N/Z_C) + \dot{I}_N}{2} e^{-\gamma x} \tag{6}$$

Suppose an arbitrary point F, which is x km away from terminal N as shown in Fig. 1*a*. The phasor of voltage at F derived from terminals N and point B are given by

$$\dot{U}_{BF} = \frac{\dot{U}_B - \dot{I}_B Z_C}{2} e^{\gamma[(1-k)\cdot l - x]} + \frac{\dot{U}_B + \dot{I}_B Z_C}{2} e^{-\gamma[(1-k)\cdot l - x]} \tag{7}$$

$$\dot{U}_{NF} = \frac{\dot{U}_N - \dot{I}_N Z_C}{2} e^{\gamma x} + \frac{\dot{U}_N + \dot{I}_N Z_C}{2} e^{-\gamma x} \tag{8}$$

where $\dot{U}_{BF}$ and $\dot{U}_{NF}$ are the voltage estimates at point F, respectively.

Since the $\dot{U}_{BF}$ is equal to $\dot{U}_{NF}$, the fault location can be expressed as [26]

$$x = (2\gamma)^{-1} \ln\left(\frac{(\dot{U}_N + \dot{I}_N Z_c) - (\dot{U}_B - \dot{I}_B Z_C) e^{\gamma(1-k)l}}{(\dot{U}_B + \dot{I}_B Z_c) e^{-\gamma(1-k)l} - (\dot{U}_N - \dot{I}_N Z_C)}\right) \tag{9}$$

2.2 Dynamic fault locator for two-terminal transmission lines

The complex quantities and angular frequency of voltage and current phasors may change rapidly under fast power oscillation condition, which will introduce some errors in the fault-location estimate. The dynamic parameter estimator method has been employed to reduce the effect is introduced as follows.

2.2.1 Dynamic parameter estimator of transmission line:

To describe the characteristics of electrical signals change along the transmission line, the equivalent series impedance and equivalent shunt admittance are defined as [26] follows

$$\tilde{Z} = R + j\omega_0 L + \frac{L}{\dot{I}(x,t)} \frac{\dot{I}(x, t+\tau) e^{-j\omega_0 \cdot \tau} - \dot{I}(x, t-\tau) e^{j\omega_0 \cdot \tau}}{2\tau} \tag{10}$$

$$\tilde{Y} = G + j\omega_0 C + \frac{C}{\dot{U}(x,t)} \frac{\dot{U}(x, t+\tau) e^{-j\omega_0 \cdot \tau} - \dot{U}(x, t-\tau) e^{j\omega_0 \cdot \tau}}{2\tau} \tag{11}$$

where $\dot{U}(x, t)$, $\dot{I}(x, t)$ and ω_0 can be measured by PMUs at two terminals of line at time t.

IET Gener. Transm. Distrib., 2016, Vol. 10, Iss. 13, pp. 3135–3141

Then, the equivalent characteristic impedance and propagation constant are given by

$$\tilde{Z}_{\mathrm{C}} = \sqrt{\tilde{Z}/\tilde{Y}} \tag{12}$$

$$\tilde{\gamma} = \sqrt{\tilde{Z} \cdot \tilde{Y}} \tag{13}$$

In this paper, the equivalent characteristic impedance and propagation constant are also used to calculate the voltage and current distributions along the line.

2.2.2 Analysis of the compensation capacity's influence: As we known, the accuracy of the voltage of SC affects the result of fault location. When the angular frequency is changing under power oscillation condition, the voltage across the SC calculated by (2) is no longer precise. In other words, it is not accurate enough to only correct the parameter of line when the fault location algorithm applied to a series transmission line. For the sake of improving the accuracy of fault location, an iteration method proposed to correct voltage across the SC. In the iteration method, an equivalent admittance ($\tilde{Y}_{\mathrm{S}}$) of the SC is defined, the derivation of $\tilde{Y}_{\mathrm{S}}$ is described as follows.

The relationship between the current ($\dot{I}_{\mathrm{S}}$) flowing through the capacitor and the voltage ($\dot{U}_{\mathrm{S}}$) across the capacitor can be expressed as

$$\dot{I}_{\mathrm{S}} = C_{\mathrm{S}} \frac{\partial \dot{U}_{\mathrm{S}}}{\partial t} \tag{14}$$

The phasors of voltage $\dot{U}_{\mathrm{S}}(x, t)$ and current $\dot{I}_{\mathrm{S}}(x, t)$ at time t are expressed by the products of a band-limited complex quantities and a constantly rotating phasor [25] $\mathrm{e}^{\mathrm{j}\omega_0 t}$ as shown in the following equations

$$\dot{U}_{\mathrm{S}}(x, t) = \dot{u}_{\mathrm{S}}(x, t)\, \mathrm{e}^{\mathrm{j}\omega_0 t} \tag{15}$$

$$\dot{I}_{\mathrm{S}}(x, t) = \dot{i}_{\mathrm{S}}(x, t)\, \mathrm{e}^{\mathrm{j}\omega_0 t} \tag{16}$$

where $\dot{u}_{\mathrm{S}}(x, t)$ and $\dot{i}_{\mathrm{S}}(x, t)$ are the band-limited complex quantities of the phasors of voltage and current, respectively, and ω_0 is the angular frequency of the constant rotating phasor.

By substituting (15) and (16) into (14), we have

$$\dot{I}_{\mathrm{S}}(x, t) = C_{\mathrm{S}} \frac{\partial \dot{U}_{\mathrm{S}}(x, t)}{\partial t} \tag{17}$$

Expanding formula (17) is shown in the following equation

$$\begin{aligned}
\dot{I}_{\mathrm{S}}(x, t) &= C_{\mathrm{S}} \frac{\partial \dot{U}_{\mathrm{S}}}{\partial t} \\
&= C_{\mathrm{S}} \frac{\partial \left(\dot{u}_{\mathrm{S}}(x, t)\, \mathrm{e}^{\mathrm{j}\omega_0 t}\right)}{\partial t} \\
&= C_{\mathrm{S}} \left(\frac{\partial \dot{u}_{\mathrm{S}}(x, t)}{\partial t} \cdot \mathrm{e}^{\mathrm{j}\omega_0 t} + \dot{u}_{\mathrm{S}}(x, t) \cdot \mathrm{j}\omega_0 \cdot \mathrm{e}^{\mathrm{j}\omega_0 t} \right) \\
&= \dot{u}_{\mathrm{S}}(x, t) \cdot \mathrm{e}^{\mathrm{j}\omega_0 t} \cdot \left(\frac{C_{\mathrm{S}}}{\dot{u}_{\mathrm{S}}(x, t)} \cdot \frac{\partial \dot{u}_{\mathrm{S}}(x, t)}{\partial t} + \mathrm{j}\omega_0 \cdot C_{\mathrm{S}} \right) \\
&= \dot{U}_{\mathrm{S}} \cdot \left(\frac{C_{\mathrm{S}}}{\dot{u}_{\mathrm{S}}(x, t)} \cdot \frac{\partial \dot{u}_{\mathrm{S}}(x, t)}{\partial t} + \mathrm{j}\omega_0 \cdot C_{\mathrm{S}} \right)
\end{aligned} \tag{18}$$

According to (18), the equivalent admittance can be defined as

$$\tilde{Y}_{\mathrm{S}} = \frac{C_{\mathrm{S}}}{\dot{u}_{\mathrm{S}}(x, t)} \cdot \frac{\partial \dot{u}_{\mathrm{S}}(x, t)}{\partial t} + \mathrm{j}\omega_0 \cdot C_{\mathrm{S}} \tag{19}$$

The $\dot{u}_{\mathrm{S}}(x, t)$ is related to the frequency. The estimate errors of $\dot{u}_{\mathrm{S}}(x, t)$ arise if considering the frequency always as a constant even under power oscillation condition. To fix that, this $\left(\partial[\dot{u}_{\mathrm{S}}(x, t)]/\partial t\right)$ is used to express the dynamic characteristics. Generally speaking, the dynamic model $(\partial[\dot{u}_{\mathrm{S}}(x, t)]/\partial t)$ will be equal to a static one if t equal to zero.

The dynamic characteristics of the voltage of the SC at report time t within a short period can be expressed by two phasor measurements at adjoining report time as shown in the following equation

$$\frac{\partial[\dot{u}_{\mathrm{S}}(x, t)]}{\partial t} = \frac{\dot{u}_{\mathrm{S}}(x, t + \tau) - \dot{u}_{\mathrm{S}}(x, t + \tau)}{2\tau} \tag{20}$$

According to (15), $\dot{u}_{\mathrm{S}}(x, t)$ can be expressed as

$$\dot{u}_{\mathrm{S}}(x, t) = \dot{U}_{\mathrm{S}}(x, t)\, \mathrm{e}^{-\mathrm{j}\omega_0 \cdot t} \tag{21}$$

By substituting (20) and (21) into (19), we have

$$\begin{aligned}
\tilde{Y}_{\mathrm{S}} &= \mathrm{j}\omega_0 \cdot C_{\mathrm{S}} + \frac{C_{\mathrm{S}}}{\dot{u}_{\mathrm{S}}(x, t)} \cdot \frac{\partial \dot{u}_{\mathrm{S}}(x, t)}{\partial t} \\
&= \mathrm{j}\omega_0 \cdot C_{\mathrm{S}} + \frac{C_{\mathrm{S}}}{\dot{U}_{\mathrm{S}}(x, t)} \frac{\dot{U}_{\mathrm{S}}(x, t + \tau)\, \mathrm{e}^{-\mathrm{j}\omega_0 \cdot \tau} - \dot{U}_{\mathrm{S}}(x, t - \tau)\, \mathrm{e}^{\mathrm{j}\omega_0 \cdot \tau}}{2\tau}
\end{aligned} \tag{22}$$

Hence, a corrected voltage drop across the SC can be obtained

$$\tilde{\dot{U}}_{\mathrm{S}} = \dot{I}_{\mathrm{S}} \cdot \frac{1}{\tilde{Y}_{\mathrm{S}}} \tag{23}$$

The flowchart of the iteration method can be illustrated in Fig. 2.

Theoretically, the more the number the iteration is, the more accuracy of the $\dot{U}_{\mathrm{S}}$ can be achieved, but more computation power is needed. Since the precise of $\dot{U}_{\mathrm{S}}$ satisfy the requirement of fault location, there is no need to sacrifice more computation power in exchange for greater accuracy. In this paper, the iteration number is one.

2.2.3 Dynamic fault locator algorithm: The fault section needs to be identified since the fault could be occurred randomly in any side of the SC. A method [29] is employed to identify the fault section. The criterion is expressed as follows

$$\begin{cases} \left|\dfrac{1}{C}\right| < \left(\dfrac{1}{C}\right)_{\mathrm{set}} & \text{fault located at the lelft-hand side of SC} \\ \left|\dfrac{1}{C}\right| > \left(\dfrac{1}{C}\right)_{\mathrm{set}} & \text{fault located at the right-hand side of SC} \end{cases} \tag{24}$$

where $1/C$ is an indicator of the fault location relative to SC, $(1/C)_{\mathrm{set}}$ is the setting, it can be set by $(1/C)_{\mathrm{set}} = 0.5 \times (1/C_{\mathrm{s}})$.

After identifying the fault section, the fault distance can be located by the follow method.

Taking Fig. 1*a* as an example, the voltage phasor at fault location derived from terminal N is given by

$$\dot{U}_{NF} = \frac{\dot{U}_N - \dot{I}_N \tilde{Z}_{NC}}{2} \mathrm{e}^{\tilde{\gamma}_N x} + \frac{\dot{U}_N + \dot{I}_N \tilde{Z}_{NC}}{2} \mathrm{e}^{\tilde{\gamma}_N x} \tag{25}$$

where $\tilde{Z}_{NC} = \sqrt{\tilde{Z}_N/\tilde{Y}_N}$ and $\tilde{\gamma}_N = \sqrt{\tilde{Z}_N \cdot \tilde{Y}_N}$.

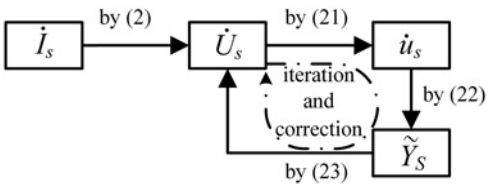

Fig. 2 *Flowchart of the iteration*

The voltage phasor at point E derived from terminal M is given as

$$\dot{U}_E = \frac{\dot{U}_M - \dot{I}_M \tilde{Z}_{MC}}{2} e^{\tilde{\gamma}_M \cdot (k \cdot l)} + \frac{\dot{U}_M + \dot{I}_M \tilde{Z}_{MC}}{2} e^{\tilde{\gamma}_M \cdot (k \cdot l)} \quad (26)$$

where $\tilde{Z}_{MC} = \sqrt{\tilde{Z}_M / \tilde{Y}_M}$ and $\tilde{\gamma}_M = \sqrt{\tilde{Z}_M \cdot \tilde{Y}_M}$, $k \cdot l$ is the distance between the SC and terminal M.

The voltage phasor at point B can be obtained

$$\dot{U}_B = \dot{U}_E - \tilde{U}_S \quad (27)$$

The voltage phasor at fault location derived from point B is given by

$$\dot{U}_{BF} = \frac{\dot{U}_B - \dot{I}_B \tilde{Z}_{BC}}{2} e^{\tilde{\gamma}_B \cdot [(1-k) \cdot l - x]} + \frac{\dot{U}_B + \dot{I}_B \tilde{Z}_{BC}}{2} e^{\tilde{\gamma}_B \cdot [(1-k) \cdot l - x]} \quad (28)$$

where $\tilde{Z}_{BC} = \sqrt{\tilde{Z}_B / \tilde{Y}_B}$ and $\tilde{\gamma}_B = \sqrt{\tilde{Z}_B \cdot \tilde{Y}_B}$.

In ideal condition, the voltage phasors of fault location derived from terminal N should be as same as the one derived from point B and the fault location is determined by

$$\dot{U}_{BF} = \dot{U}_{NF} \quad (29)$$

Newton iterative method is employed to solve the non-linear (29). When it comes to a three-phase transmission lines, the positive-sequence component is employed in all the formulas. In the proposed method, the positive-sequence component is obtained for the three-phase system through the inverse transformation of symmetrical components.

2.3 Program of proposed method

Also, taking Fig. 1*a* as an example, the overall flowchart of the proposed fault-location algorithm after identifying the fault section is shown in Fig. 3, the specific steps are introduced as follows:

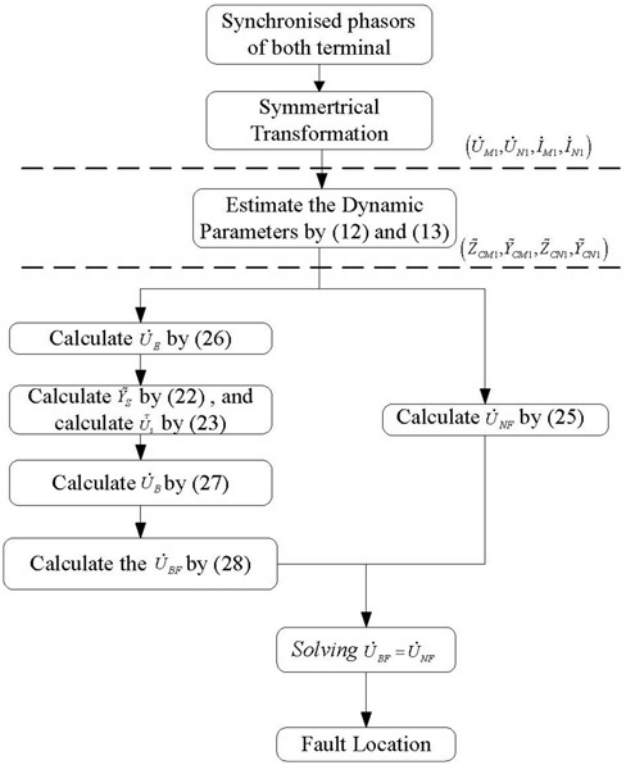

Fig. 3 *Flowchart of the proposed algorithm*

Step 1: Obtain the positive sequence components of current and voltage signals through the inverse transformation of symmetrical components after getting the phasor estimate from PMUs. All quantities, if not specifically labelled, refer to positive-sequence quantities.

Step 2: Obtain the voltage of fault point ($\dot{U}_{NF}$) from terminal N by (25).

Step 3: Calculate the voltage ($\dot{U}_E$) and current ($\dot{I}_E$) of point E by (26).

Step 4: Obtain $\tilde{Y}_S$ based on $\dot{U}_S$ by (22), then correct the voltage across the SC ($\tilde{U}_S$) by (23).

Step 5: Obtain the voltage of fault point ($\dot{U}_{BF}$) from point B by (28).

Step 6: Employ Newton iteration to estimate the fault location.

3 Performance evaluation

The proposed method has been simulated on a 500-kV, 300 km and transmission network with a SC compensated transmission line. The transmission line is depicted in Fig. 4. The parameters of line are shown as follows: $C_S = 100$ μF, $R_1 = 0.034676$ Ω/km, $L_1 = 1.347616$ mH/km, $G_1 = 1.0 \times 10^{-7}$ S/km and $C_1 = 8.6771 \times 10^{-9}$ F/km. $R_0 = 0.300023$ Ω/km, $L_0 = 3.63714$ mH/km and $C_0 = 6.16105 \times 10^{-9}$ μF/km. The power system is modelled in terms of distributed parameters and simulated using the PSCAD/EMTDC, and the Matlab software is employed to verify the adaptability of the proposed algorithm. In all the cases, the frequency of power system is 50 Hz, and the voltage and current signals sampled at a rate of 2.4 kHz. That is to say, 48 samples per cycle. The dynamic phasor estimation algorithm is employed to estimate the phasors of voltage and current signals. The report rate is set to 50 Hz. The slip window length is one cycle. A disturbance introduced to the source M at 1.5 s, which brings power oscillation condition. Steady fault location algorithm (SFLA) is employed as a comparison method to evaluate the performance of dynamic fault location algorithm for series-capacitor compensated transmission line proposed in this paper which abbreviated as DFLSC. Besides, the simulation of dynamic fault location algorithm without correcting the voltage across the SC which abbreviated as DFLA is also appeared to verify the effectiveness of the proposed algorithm. AFL represents the actual fault location index away from the end of the faulted line section.

In these simulation studies, the estimate error of the fault location methods is calculated as

$$\text{Error}(\%) = \frac{|x - x_{\text{Actual}}|}{L} \times 100 \quad (30)$$

where x_{Actual} is the theoretical value of fault location.

Taking the complex frequency components introduced by fault into account, the measured three-phase voltage and current signals are filtered using a pre-bandpass filter with centre frequency of 50 Hz. The simulation result is organised as follows. Under the assumption that fault occurs on the right-hand side of the SC, parts A and B mainly verify the adaptation of the proposed method considering the fault type, fault distance and fault resistance, respectively. Part C discusses the effectiveness of the proposed method when the fault occurs on the left-hand side of SC with different fault type, different resistance and different location.

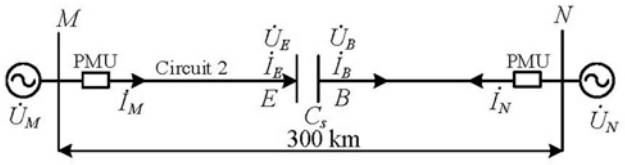

Fig. 4 *Model of power system*

IET Gener. Transm. Distrib., 2016, Vol. 10, Iss. 13, pp. 3135–3141

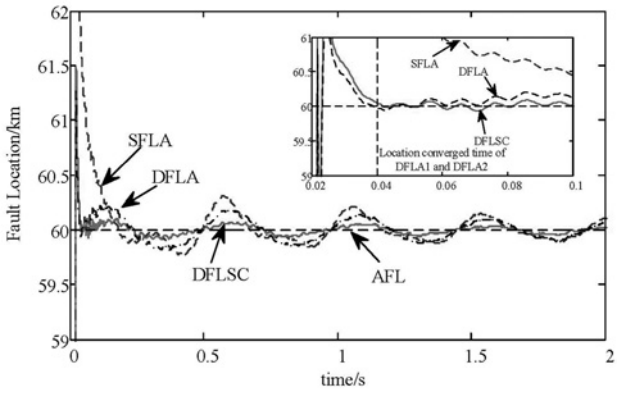

Fig. 5 *Fault location estimate of three algorithms under an ABC-G fault (fault resistance: 100 Ω; fault distance: 60 km)*

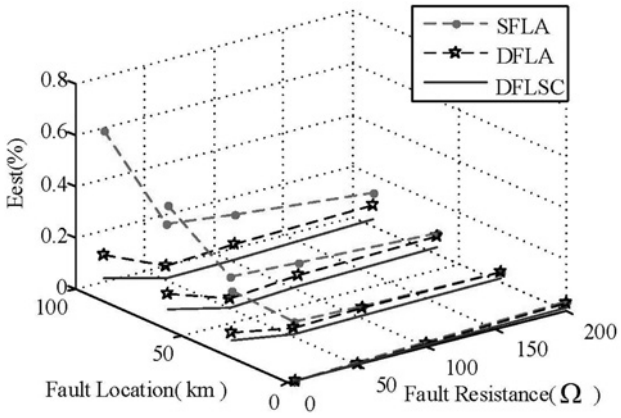

Fig. 7 *Estimate errors of three algorithms under ABC fault with different fault resistances at different distances*

3.1 Cases with different fault location and fault resistance

Fig. 5 shows the fault-location of estimates of SFLA, DFLA and DFLSC. The three-phases-to-ground fault (fault resistance: 100 Ω; fault distance: 60 km) occurs at 0 s. In order to show a better performance, the fault data used in the simulation is 2 s. To deal with those data, the computation time is 0.747 s. In addition, it can be concluded that without considering the dynamic characteristics of voltage and current, the estimate of SFLA turns aside considerably from the AFL in the form of oscillation compared to DFLA and DFLSC. Furthermore, compared the algorithms between DFLSC and DFLA, it is found that the estimate of DFLSC is smoother than DFLA because of considering the influence the changing frequency has on the SC. From the perspective of the convergence time, considering the effect introduced by the power oscillation is beneficial to shorten the convergence time. As shown in Fig. 5, the convergence time of DFLA and DFLSC are about 40 ms, whereas SFLA costs 70 ms. Even though the voltage drop across the SC is corrected, some small oscillation exists in the estimate of DFLSC because the initial value of capacitor voltage does exist error. The estimate error is also introduced by the Taylor error of the signal model, however, it will not discussed in this paper since it have been discussed in detail [26].

Fig. 6 and Table 1 show the absolute errors and the estimate errors of three algorithms under ABC-G fault with different fault resistances (5, 10, 100 and 200 Ω) at different distances (0, 30, 60 and 90 km), respectively. It is concluded that the mean error of SFLA fluctuates in a larger scope, the maximum estimate error of DFLSC can be kept within 0.1372% whereas that of SFLA increases up to 0.7930% and DFLA increases up to 0.3256%. Moreover, the error estimate of DFLA is close to SFLA in most cases. The reasons can be concluded from two aspects. On the one hand, it has taken full consideration of dynamic characteristics

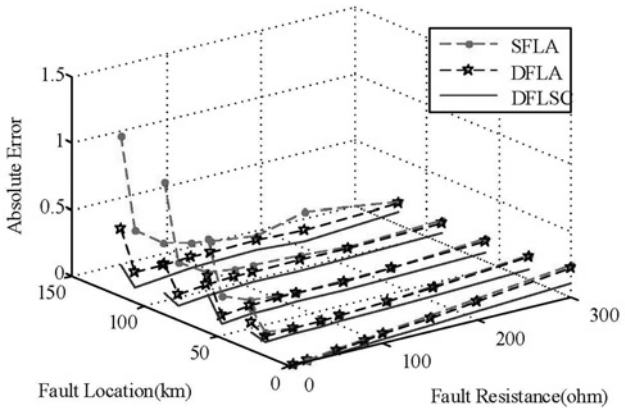

Fig. 6 *Absolute errors of three algorithms under ABC-G fault with different fault resistances at different distances*

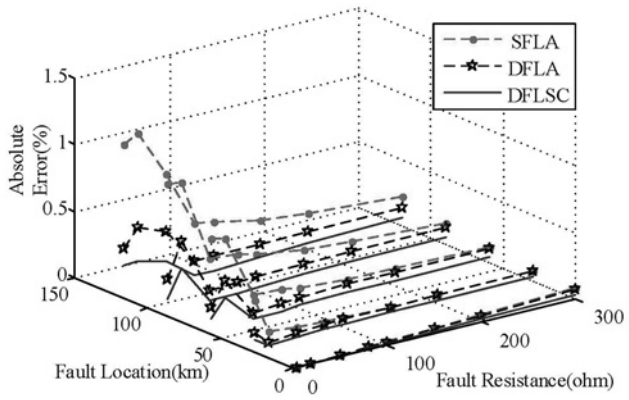

Fig. 8 *Absolute errors of three algorithms under ABC fault with different resistances at different distances*

Table 1 Mean errors of estimate under ABC-G fault with different fault locations and different fault resistances

Actual fault location, km	E_{est}(%)											
	$R_f = 5\ \Omega$			$R_f = 50\ \Omega$			$R_f = 100\ \Omega$			$R_f = 200\ \Omega$		
	SFLA	DFLA	DFLSC	SFLA	DFLA	DFLSC	SFLA	DFLA	DFLA	SFLA	DFLA	DFLSC
0	0.0027	0.0027	0.0011	0.0267	0.0240	0.0107	0.0544	0.0488	0.0226	0.1070	0.0959	0.0434
30	0.1966	0.1223	0.0788	0.0432	0.0419	0.0159	0.0471	0.0465	0.0180	0.0780	0.0755	0.0302
60	0.4560	0.2683	0.1738	0.0924	0.0683	0.0246	0.0741	0.0690	0.0266	0.0840	0.0781	0.0318
90	0.6490	0.2369	0.0910	0.1440	0.0772	0.0247	0.1083	0.0868	0.0353	0.0930	0.0871	0.0382
120	0.7930	0.3256	0.1372	0.2033	0.0851	0.0221	0.1517	0.0943	0.0413	0.1054	0.0957	0.0494

Table 2 Mean errors of estimate under different fault type, different fault resistances and different locations

Fault type	Actual fault location, km	E_{est}, %											
		$R_f = 5\ \Omega$			$R_f = 50\ \Omega$			$R_f = 100\ \Omega$			$R_f = 200\ \Omega$		
		SFLA	DFLA	DFLSC	SFLA	DFLA	DFLSC	SFLA	DFLA	DFLSC	SFLA	DFLA	DFLSC
A-G	0	0.0082	0.0075	0.0033	0.0801	0.0717	0.0323	0.1614	0.1441	0.0661	0.3231	0.2890	0.1325
	30	0.1131	0.0304	0.0141	0.1405	0.0773	0.0263	0.2000	0.1377	0.0506	0.3317	0.2753	0.1092
	60	0.2121	0.0548	0.0296	0.2341	0.0964	0.0339	0.2546	0.1330	0.0482	0.3614	0.2574	0.1143
	90	0.2960	0.0773	0.0437	0.3305	0.1132	0.0431	0.3206	0.1447	0.0583	0.3860	0.2703	0.1521
	120	0.3639	0.0949	0.0557	0.4208	0.1266	0.0529	0.3870	0.1596	0.0731	0.4031	0.2911	0.2121
BC	0	0.0028	0.0027	0.0011	0.0272	0.0245	0.0113	0.0540	0.0485	0.0224	0.1074	0.0962	0.0445
	30	0.0463	0.0154	0.0131	0.0811	0.0448	0.0116	0.0715	0.0511	0.0204	0.0988	0.0808	0.0321
	60	0.2650	0.0753	0.0353	0.1755	0.0641	0.0276	0.1487	0.0795	0.0322	0.1289	0.0869	0.0494
	90	0.5034	0.1690	0.0694	0.2386	0.0736	0.0415	0.2379	0.1022	0.0442	0.1789	0.1047	0.0515
	120	0.7368	0.2516	0.1798	0.2865	0.0900	0.0565	0.3092	0.1191	0.0603	0.2364	0.1266	0.0672
BC-G	0	0.0041	0.0039	0.0016	0.0399	0.0358	0.0162	0.0813	0.0728	0.0336	0.1629	0.1459	0.0676
	30	0.0485	0.0134	0.0094	0.0670	0.0464	0.0167	0.0797	0.0632	0.0243	0.1368	0.1207	0.0476
	60	0.3891	0.1329	0.0718	0.1497	0.0765	0.0247	0.1203	0.0786	0.0290	0.1425	0.1072	0.0430
	90	0.7404	0.2175	0.0889	0.2260	0.0941	0.0331	0.1754	0.0995	0.0385	0.1624	0.1128	0.0503
	120	0.9610	0.3631	0.2062	0.2863	0.1059	0.0394	0.0434	0.1176	0.0496	0.1850	0.1269	0.0669

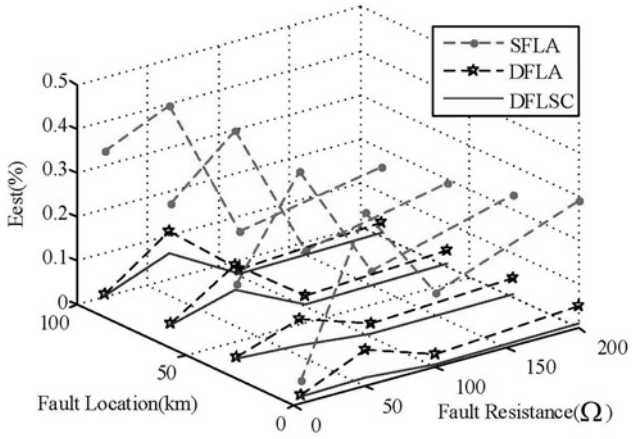

Fig. 9 *Mean errors of three algorithms under ABC fault with different fault resistances at different distances*

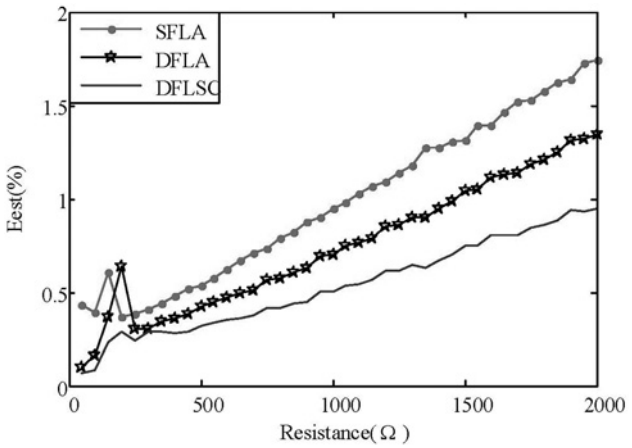

Fig. 11 *Mean errors of three algorithms under A-G fault with different resistances when the fault location is 60 km*

compared with the SFLA. On the other hand, the iteration method is used to eliminate the error brought by the voltage of the SC compared with the DFLA. As a result, it is not accurate enough to only consider the impact of the dynamic characteristics of signals, which means, the iteration method is also necessary and effective.

Meanwhile, it's observed that the average errors of all algorithms increase as the fault location increases. Theoretically, the error should increase as the fault resistance increases. The reason why the error of the cases with 0 and/or 5 Ω fault resistances are higher than others is that these faults create vital disturbance to the power system so that the power system becomes unstable soon after fault. The power system collapse is totally out of the scope of this paper because the phasor of voltage and current cannot be extracted accurately.

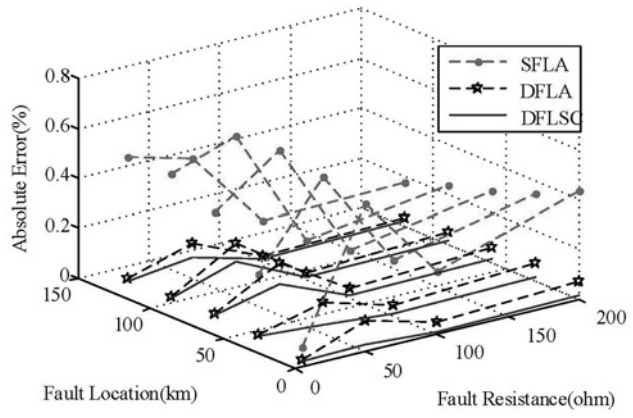

Fig. 10 *Absolute errors of three algorithms under ABC fault with different resistances at different distances*

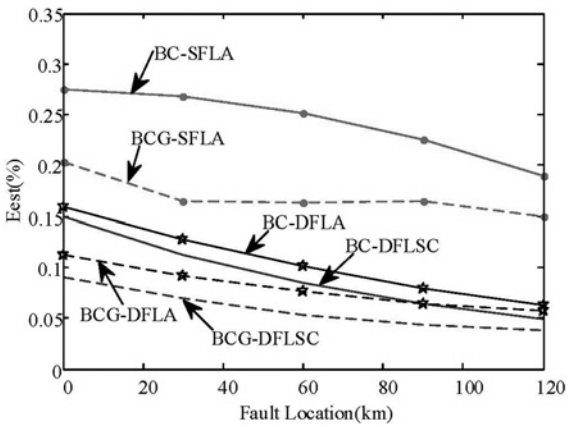

Fig. 12 *Mean errors of fault location estimate of three algorithms under different fault types and different distances, when the fault resistance is 100 Ω*

IET Gener. Transm. Distrib., 2016, Vol. 10, Iss. 13, pp. 3135–3141

3.2 Cases with different fault types and fault resistances

Figs. 7 and 8 show the fault location estimate errors and the absolute errors of three algorithms under three-phase fault with different fault resistances at different fault distances. It can be observed that the DFLSC shares minimum error among the three algorithms, and it is independent of the fault resistance. As the fault resistance increases, the error estimate of DFLA is close to SFLA.

The estimate error of three algorithms under single-phase ground fault (A-G), two-phase fault (BC) and two-phase ground fault (BC-G) with different fault resistances and different distances are shown in Table 2. The results show that the proposed method has a better performance than SFLA and DFLSC, the maximum estimate error of DFLSC is under 0.2121% in all the fault types. However, the maximum estimate error of DFLA increases up to 0.3631% and that of SFLA increases up to 0.9610%.

3.3 Case with fault occurred on the left-hand side of series capacitor

Figs. 9–12 describe the performance of three algorithms when the fault occurs on the left-hand side of the SC. Fig. 9 describes the estimate errors of three algorithms under ABC fault with different distances and different resistances. Fig. 10 shows the absolute errors of three algorithms under ABC fault with different fault resistances at different distances. Fig. 11 shows the estimate errors of three algorithms under A-G fault with different fault resistances. Fig. 12 shows the estimate errors of three algorithms under BC-G fault and BC fault with different fault distances. It can be easily observed that the fault location estimates of DFLSC are more accurate than the other two algorithms and virtually independent of the fault resistance even the fault occurs on the left-hand side of SC.

4 Conclusions

This paper proposes a novel fault location algorithm for SC compensated transmission line under dynamic conditions by using synchronised phasor measurements obtained by PMUs. The influence on the SC caused by power oscillation has been fully considered by DFLSC. The algorithm gives better fault localisation estimate under power oscillation condition with comparison to the fault location algorithms which did not consider the dynamic characteristics of line or the SC.

The performance of the proposed method has been evaluated with diverse faults on a 500 kV SC compensated transmission line. PSCAD/EMTDC software was used to generate fault signals in different fault distances, fault types and fault resistance. The evaluation results have verified that the estimate errors of fault location induced from the incorrect of the voltage of SC can be eliminated in some degree by the proposed method, which has a better performance than the conventional algorithms under power oscillation conditions. However, the proposed algorithm needs to identify fault location by another method, exploring a more consummate location scheme to this problem is the next step of this research.

5 Acknowledgment

This work is supported by National Natural Science Foundation of China (51307145, 51307146), and the Application Basic Research Project of Sichuan Province (No. 2014JY0177).

6 References

1 Sarangi, S., Pradhan, A.K.: 'Synchronised data-based adaptive backup protection for series compensated line', *IET Gener. Transm. Distrib.*, 2014, **8**, (12), pp. 1979–1986

2 Xu, Z.Y., Su, Z.P., Zhang, J.H., *et al.*: 'An interphase distance relaying algorithm for series-compensated transmission lines', *IEEE Trans. Power Deliv.*, 2014, **29**, (2), pp. 834–841

3 Jiang, Q., Li, X., Wang, B., *et al.*: 'PMU-based fault location using voltage measurements in large transmission networks', *IEEE Trans. Power Deliv.*, 2012, **27**, (3), pp. 1644–1652

4 Saha, M.M., Izykowski, J., Rosolowski, E., *et al.*: 'A new accurate fault locating algorithm for series compensated lines', *IEEE Trans. Power Deliv.*, 1999, **14**, (3), pp. 789–797

5 Razzaghi, R., Lugrin, G., Paolone, M., *et al.*: 'On the use of electromagnetic time reversal to locate faults in series-compensated transmission lines'. 2013 IEEE Grenoble PowerTech Conf., 2013, pp. 1–5

6 Al-Mohammed, A.H., Abido, M.A.: 'A fully adaptive pmu-based fault location algorithm for series-compensated lines', *IEEE Trans. Power Deliv.*, 2014, **29**, (5), pp. 2129–2137

7 Jafarian, P., Sanaye-Pasand, M.: 'High-speed superimposed-based protection of series-compensated transmission lines', *IET Gener. Transm. Distrib.*, 2011, **5**, (12), pp. 1290–1300

8 Swetapadma, A., Yadav, A.: 'Improved fault location algorithm for multi-location faults, transforming faults and shunt faults in thyristor controlled series capacitor compensated transmission line', *IET Gener. Transm. Distrib.*, 2015, **9**, (13), pp. 1597–1607

9 Ray, P., Panigrahi, B.K., Senroy, N.: 'Hybrid methodology for fault distance estimation in series compensated transmission line', *IET Gener. Transm. Distrib.*, 2013, **7**, (5), pp. 431–439

10 Razzaghi, R., Lugrin, G., Manesh, H., *et al.*: 'An efficient method based on the electromagnetic time reversal to locate faults in power networks', *IEEE Trans. Power Deliv.*, 2013, **28**, (3), pp. 1663–1673

11 Ahsaee, M.G., Sadeh, J.: 'A novel fault-location algorithm for long transmission lines compensated by series FACTS devices', *IEEE Trans. Power Deliv.*, 2011, **26**, (4), pp. 2299–2308

12 Sadeh, J., Hadjsaid, N., Ranjbar, A.M., *et al.*: 'Accurate fault location algorithm for series compensated transmission lines', *IEEE Trans. Power Deliv.*, 2000, **15**, (3), pp. 1027–1033

13 Yu, C.-S., Liu, C.-W., Jiang, J.-A.: 'A new fault location algorithm for series compensated lines using synchronized phasor measurements'. Power Engineering Society, IEEE Summer Meeting, Seattle, WA, July 2000, pp. 1350–1354

14 Izykowski, J., Rosolowski, E., Balcerek, P., *et al.*: 'Accurate noniterative fault location algorithm utilizing two-end unsynchronized measurements', *IEEE Trans. Power Deliv.*, 2010, **25**, (1), pp. 72–80

15 Rubeena, R., Mohammad, R., Zadeh, D., *et al.*: 'An accurate offline phasor estimation for fault location in series-compensated lines', *IEEE Trans. Power Deliv.*, 2014, **29**, (2), pp. 876–883

16 Bains, T.P.S., Dadash Zadeh, M.R.: 'Enhanced phasor estimation technique for fault location in series compensated lines', *IEEE Trans. Power Deliv.*, 2015, **30**, (4), pp. 2058–2060

17 Saha, M., Izykowski, J., Rosolowski, E.: 'Fault location method using measurements of differential relays for parallel transmission lines with series capacitor compensation at both ends'. Proc. Int. Conf. Developments in Power Systems Protection (DPSP), Birmingham, UK, April 2012, pp. 1–6

18 Kang, N., Chen, J., Liao, Y.: 'A fault-location algorithm for series-compensated double-circuit transmission lines using the distributed parameter line model', *IEEE Trans. Power Deliv.*, 2015, **30**, (1), pp. 360–367

19 Mechraoui, A., Thomas, D.W.P.: 'A new principle for high resistance earth fault detection during fast power swings for distance protection', *IEEE Trans. Power Deliv.*, 1997, **12**, (4), pp. 1452–1457

20 He, Z., Fu, L., Han, W., *et al.*: 'Precise algorithm for frequency estimation under dynamic and step-change conditions', *IET Sci. Meas. Technol.*, 2015, **9**, (7), pp. 842–851

21 Nayak, P.K., Pradhan, A., Bajpai, P.: 'A fault detection technique for the series-compensated line during power swing', *IEEE Trans. Power Deliv.*, 2013, **28**, (2), pp. 714–722

22 Moravej, Z., Pazoki, M., Khederzadeh, M.: 'Impact of UPFC on power swing characteristic and distance relay behavior', *IEEE Trans. Power Deliv.*, 2014, **29**, (1), pp. 261–268

23 Khorashadi-Zadeh, H.: 'Evaluation and performance comparison of power swing detection algorithms'. IEEE Power and Energy Society General Meeting, 2005, pp. 1842–1848

24 Mai, R., He, Z., Fu, L., *et al.*: 'A dynamic synchrophasor estimation algorithm for online application', *IEEE Trans. Power Deliv.*, 2010, **25**, (2), pp. 570–578

25 Mai, R., He, Z., Fu, L., *et al.*: 'Dynamic phasor and frequency estimator for phasor measurement units', *IET Gener. Transm. Distrib.*, 2010, **4**, (1), pp. 73–83

26 He, Z., Mai, R., He, W., *et al.*: 'Phasor-measurement-unit-based transmission line fault location estimator under dynamic conditions', *IET Gener. Transm. Distrib.*, 2011, **5**, (11), pp. 1183–1191

27 He, Z., Li, X., He, W., *et al.*: 'Dynamic fault locator for three-terminal transmission lines for phasor measurement units', *IET Gener. Transm. Distrib.*, 2013, **7**, (2), pp. 183–191

28 Song, G., Chu, X., Gao, S., *et al.*: 'Novel distance protection based on distributed parameter model for long-distance transmission lines', *IEEE Trans. Power Deliv.*, 2013, **28**, (4), pp. 2116–2123

29 Wang, Y., Yin, X., Zhang, Z., *et al.*: 'A new method for identifying the fault location on series compensated lines based on transient fault information'. Proc. Int. Conf. Developments in Power Systems Protection (DPSP), Weihai, Shandong, July 2011, pp. 78–82

30 Kundur, P., Balu, N.J., Lauby, M.G.: 'Power system stability and control' (McGraw-hill, New York, 1994)